Supplementary Materials

Table S1. Peak values and R squares of the average density distribution of 50, 100, 200, and 400 nm particles at 20 °C (room temperature), 150 °C, and 300 °C.

	50 nm			100 nm			200 nm			400 nm		
	x_{c1}	x_{c2}	R^2	x_{c1}	x_{c2}	R^2_1	x_{c1}	x_{c2}	R^2	x_{c1}	x_{c2}	R^2
20°C	1.167	\	0.980	0.933	1.454	0.979	0.939	1.519	0.9697	1.344	1.917	0.966
150 °C	0.972	1.642	0.951	0.981	1.691	0.932	0.984	1.746	0.949	1.094	1.798	0.911
300 °C	0.976	1.756	0.851	0.994	1.851	0.864	1.030	1.857	0.850	1.157	2.051	0.779

Table S2. Single scattering albedo (SSA) at wavelengths of 530 nm and 450 nm and Ångström absorption exponent (AAE) of total biomass burning particles at 20 °C (room temperature), 150 °C, and 300 °C.

Temperature	SSA		AAE
	450 nm	530 nm	
Room temperature (20 °C)	0.750	0.897	6.230±0.160
150 °C	0.533	0.723	5.047±0.246
300 °C	0.469	0.560	2.229±0.292

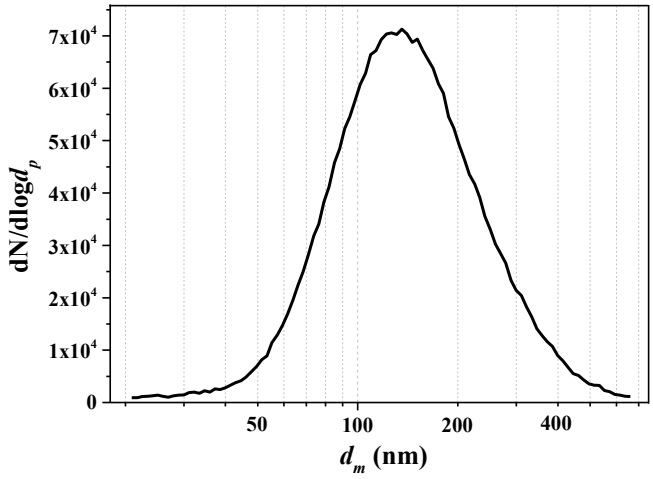

Figure S1. Average number size distribution of biomass burning particles.

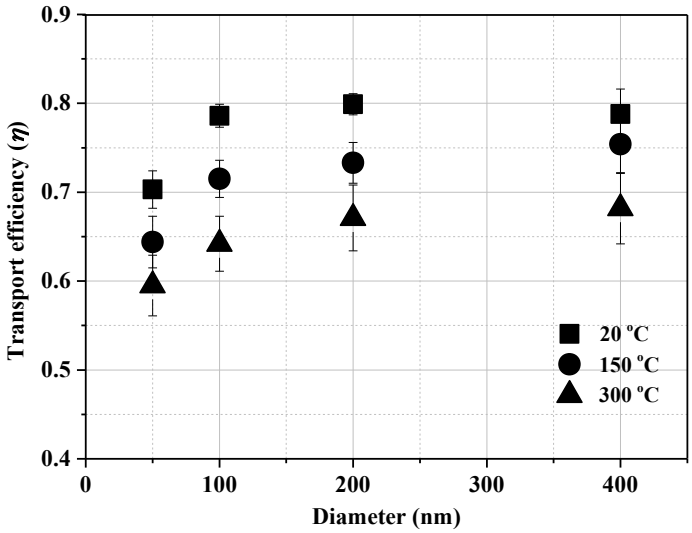

Figure S2. Transport efficiency of NaCl in the thermodenuder as a function of particle diameter and heating temperature.

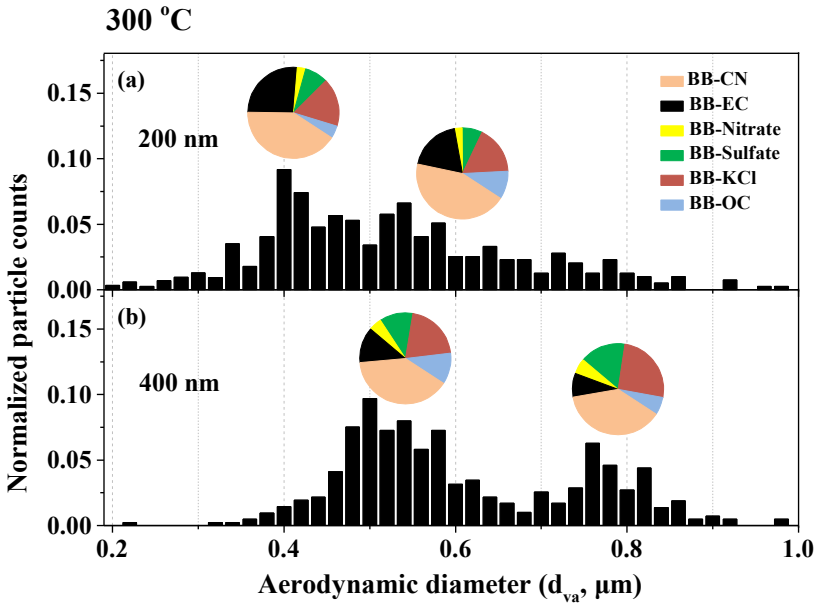

Figure S3. Vacuum aerodynamic size distributions detected by the SPAMS of 200 nm and 400 nm electrical mobility size-selected biomass burning particles and pie charts for the particle types in different aerodynamic modes at 300 °C.

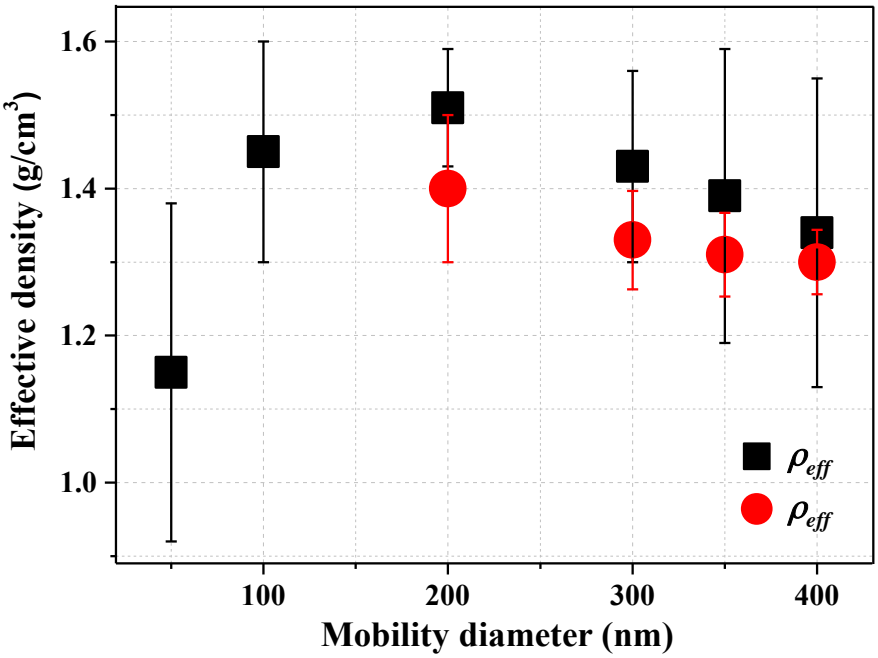

Figure S4. Size-resolved effective density of biomass burning particles determined by two methods. ρ_{eff}^{I} is effective density from mobility and mass measurements (based on the DMA-APM-CPC system) while ρ_{eff}^{II} is from mobility and aerodynamic measurements (DMA-SPAMS system). The effective density of each size is the average peak value of the dominant mode from different scans. Error bars represent the standard deviations of the five replicate test results.

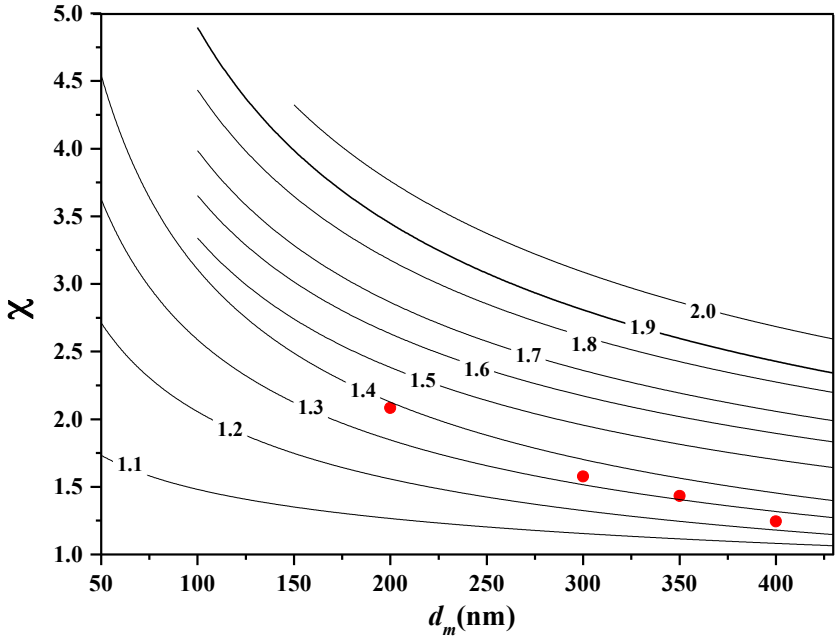

Figure S5. Contour plot of the ratio of the estimated particle mass (m_p) to the exact m_p. The estimated m_p was obtain by replacing ρ_{eff}^{I} with calculated ρ_{eff}^{II} in Equation (2). The ratios of the estimated m_p by replacing ρ_{eff}^{I} with exact ρ_{eff}^{II} in Equation (2) to the exact m_p was shown as well (red dots).

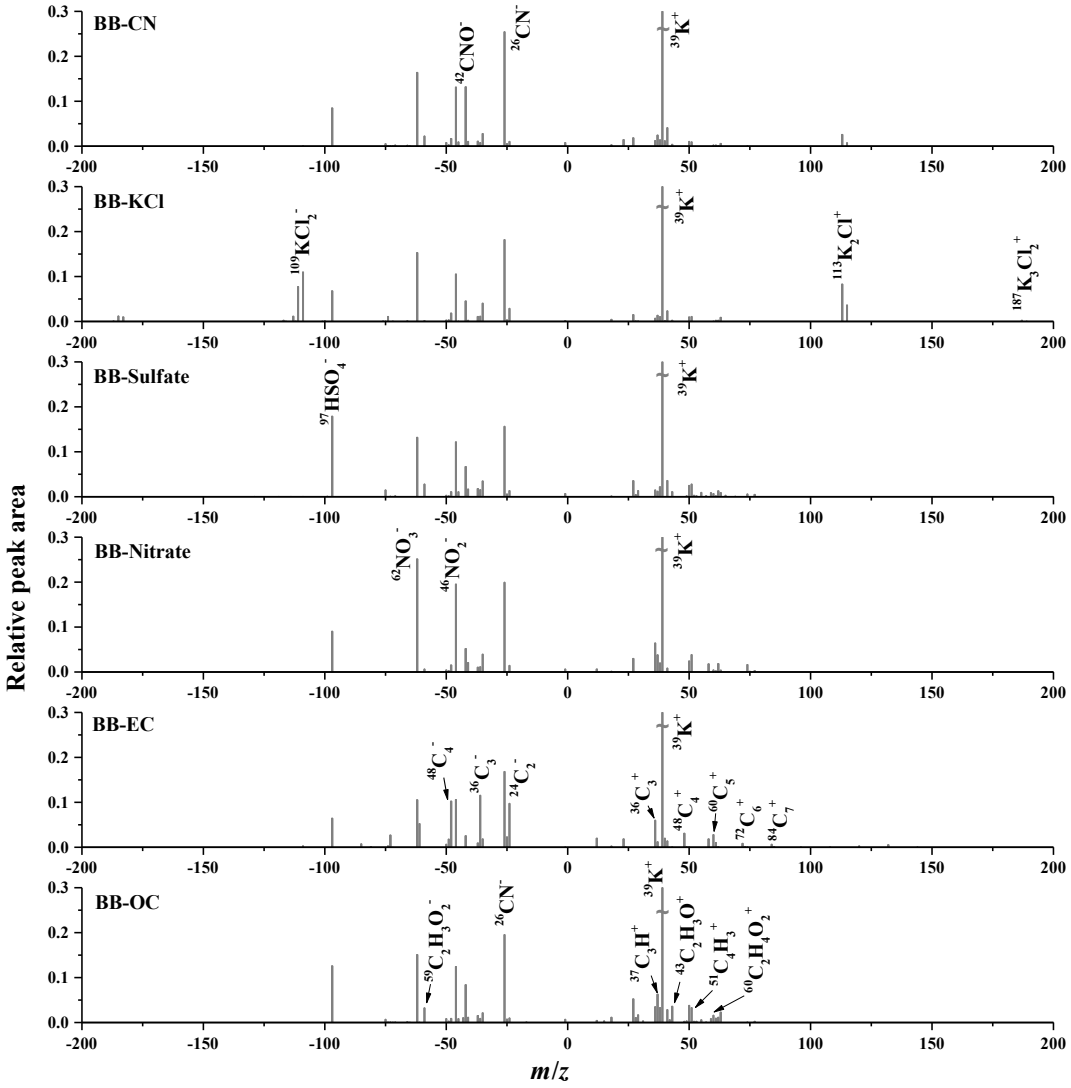

Figure S6. Average mass spectra of 6 particle types classified from biomass burning particles.

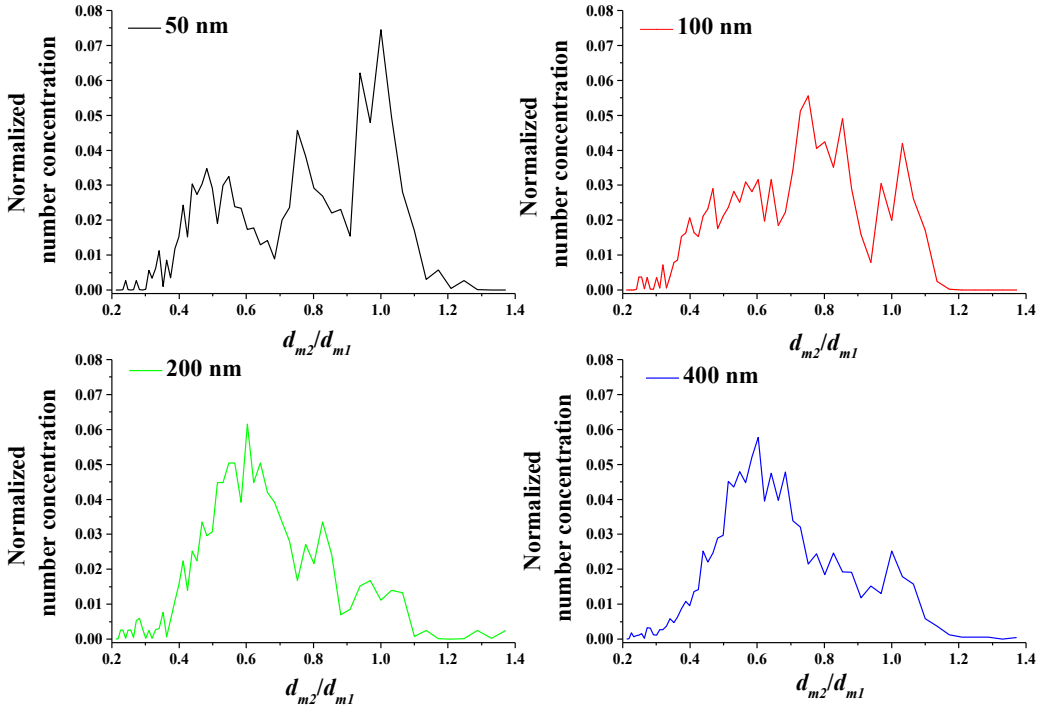

Figure S7. The size change (d_{m2}/ d_{m1}) for particles in the size range of 50-400 nm when heated at 300 ^{o}C.